Journal of Sound and Vibration (2000) **233**(1), 81–92
doi:10.1006/jsvi.1999.2792, available online at http://www.idealibrary.com on IDEAL®

STOCHASTIC RESPONSE OF BASE-EXCITED COULOMB OSCILLATOR

G.-K. ER AND V. P. IU

Faculty of Science and Technology, University of Macau, P.O. Box 3001, Macau

(*Received* 2 *December* 1998, *and in final form* 19 *November* 1999)

The probabilistic solution to the stochastic responses of a rigid structure connected to a foundation with Coulomb friction-type base isolation subjected to stationary Gaussian white-noise-type ground excitations is investigated. The base isolation system which can be described with a base-excited Coulomb oscillator utilizes sliding bearing in which the coefficient of friction exhibits strong dependence on the sliding velocity. The analytical probabilistic solutions are obtained with both an equivalent linearization procedure and a new method proposed recently. The analytical solutions are verified by Monte Carlo simulation and the results show that the method utilized yields better solutions than the equivalent linearization procedure. It is also found that friction-type base isolation systems exhibit softening non-linearity and the method utilized is well suited to systems with softening non-linearity.

1. INTRODUCTION

The use of base isolation systems has gained popularity in earthquake-resistant design of building structures. The basic mechanism is to isolate strong ground motion induced by earthquake from the structure by introducing flexibility and energy-absorption capacity. Various isolation systems have been proposed and reviewed in the literature [1–4] and the responses of base-isolation system have attracted considerable investigation [5–10]. Previous analytical studies of the stochastic responses adopt mainly the equivalent linearization procedure. It is known that the equivalent linearization procedure is only effective for weakly non-linear systems as in the case of sliding isolation systems. Moreover, the equivalent linearization procedure leads to Gaussian probability density function (PDF) of system responses, which is not correct for non-linear systems. If Gaussian PDF is still utilized for the probability evaluation or some other statistical analysis such as higher moment evaluation and reliability analysis of structures, the results can be much distorted. Therefore, more accurate PDF solutions are desirable. In past decades, much attention was paid to the improved PDF solution of non-linear stochastic systems based on various methods though some restrictions are inherent in them. Recently, a new method which may be called local weighted residual method in the following statement for the PDF analysis of non-linear stochastic systems, was proposed and applied to some non-linear systems [11–13]. The method is free of the degree of non-linearity of systems. In this paper, the PDF of the sliding base-isolation system with Coulomb friction force under the action of horizontal ground motion is analyzed with the new method. The results obtained with this method are compared with those from the equivalent linearization procedure and Monte Carlo simulation to verify the effectiveness of the method for this base-isolation system subjected to horizontal ground excitations.

2. MATHEMATICAL MODEL OF SLIDING BASE ISOLATION SYSTEM

The resilient-friction base isolator (R-FBI) which was found to have the broadest range of applicability was investigated by many researchers [10]. This isolator consists of concentric layers of Teflon-coated plates that are in friction contact with each other and contains a central core of rubber of steel-reinforced laminated rubber. A rubber bearing and a pure-friction isolator in parallel are used in the base-isolation design. In the analysis of base-isolation system, the upper structure is usually assumed to be rigid with mass m. The base-isolated system is assumed to consist of a spring with stiffness k and a dashpot with damping constant c. The moving upper structure is in contact with the spring and dashpot. When the mass is in motion, Coulomb friction force is developed which is imposed on the mass. The equation of motion for the mass can take the following form:

$$m\ddot{X}(t) + c\dot{X}(t) + \mu mg\,\mathrm{sign}(\dot{X}) + kX(t) = mg\ddot{X}_g(t), \tag{1}$$

where μ is the coefficient of sliding friction, g is the gravitational acceleration, sign $(\cdot)$ denotes the sign function and $\ddot{X}_g(t)$ is the relative acceleration of ground motion to gravitational acceleration, which is assumed to be stationary Gaussian white noise with

$$E[\ddot{X}_g(t+\tau)\ddot{X}_g(t)] = S\delta(\tau), \tag{2}$$

where $\delta(\tau)$ is Dirac Delta function.

Equation (1) may also be written in the following form:

$$\ddot{X}(t) + 2\xi\omega\dot{X}(t) + \mu g\,\mathrm{sign}(\dot{X}) + \omega^2 X(t) = g\ddot{X}_g(t), \tag{3}$$

where ξ is damping ratio and ω is the linear natural frequency of the system. It is obvious that equation (3) expresses a strongly non-linear system because the value of sliding friction coefficient μ is usually around 0·1 and therefore, the value of $g\mu$ is around 1 m/s^2. In this paper, the PDF solutions of the system are investigated with both the equivalent linearization procedure and the local weighted residual method, and the results are compared with those obtained by Monte Carlo simulation in the following sections. Some behaviors of the solutions are observed which provide some information about the structure responses and the effectiveness of the local weighted residual method for the system whose PDF solutions are similar to those of the friction-type sliding systems.

3. EQUIVALENT LINEARIZATION PROCEDURE

The solution of equation (3) was studied with the equivalent linearization procedure but only the variances of the responses were compared with those by Monte Carlo simulation. Because of the importance of PDFs in reliability analysis, it is also necessary to predict the PDFs of system responses. If equation (3) is replaced by the linear equation

$$\ddot{X}(t) + 2\xi_e\omega_e\dot{X}(t) + \omega_e^2 X(t) = g\ddot{X}_g(t), \tag{4}$$

then the response of equation (4) is Gaussian and the PDF of the responses from equation (4) can be determined with the variances of the responses. With the equivalent linearization procedure and observing that for stationary, Gaussian zero-mean input process $\ddot{X}_g(t)$, responses $X(t)$ and $\dot{X}(t)$ are Gaussian processes and in a stationary state and are uncorrelated. ξ_e and ω_e can be obtained in a stationary state as

$$\omega_e = \omega, \qquad \xi_e = \xi + \frac{\mu g}{\sqrt{2\pi}\omega\sigma_{\dot{X}}}, \tag{5, 6}$$

where $\sigma_{\dot{X}}$ is the variance of $\dot{X}$.

For system (4), the variances of stationary X and $\dot{X}$ are given by

$$\sigma_X^2 = \frac{S}{4\xi_e\omega^3}, \qquad \sigma_{\dot{X}}^2 = \frac{S}{4\xi_e\omega}, \tag{7, 8}$$

Solving equations (6)–(8) leads to

$$\sigma_{\dot{X}} = \frac{\sqrt{(\mu g)^2 + 2\pi\xi\omega S} - \mu g}{2\sqrt{2\pi}\xi\omega}, \tag{9}$$

$$\sigma_X = \frac{1}{2}\left[\frac{S}{\xi + \mu g/\sqrt{2\pi}\omega^3\sigma_{\dot{X}}}\right]^{1/2} \tag{10}$$

for which the PDF of X and $\dot{X}$ can be obtained as

$$p(x, \dot{x}) = \frac{1}{2\pi\sigma_x\sigma_{\dot{x}}}\exp\left(-\frac{x^2}{2\sigma_x^2} - \frac{\dot{x}^2}{2\sigma_{\dot{x}}^2}\right) \tag{11}$$

which is the PDF solution of system responses resulting from the equivalent linearization procedure.

4. NEW PROCEDURE

In this section, the PDF solution of the responses of system (3) is obtained with the local weighted residual method [11–13].

Setting $X_1 = X$ and $X_2 = \dot{X}$, equation (3) is written in Ito's form as follows:

$$\dot{X}_1 = X_2, \qquad \dot{X}_2 = f(X_1, X_2) + g\ddot{X}_g(t), \tag{12, 13}$$

where

$$f(X_1, X_2) = -2\xi\omega X_2 - \mu g\,\mathrm{sign}(X_2) - \omega^2 X_1. \tag{14}$$

The response, $\{X_1, X_2\} \in \Re^2$ where $\Re$ denotes real space, is a Markov vector and the probability density of the stationary Markov vector is governed by the reduced FPK equation

$$x_2\frac{\partial p(x_1, x_2)}{\partial x_1} + \frac{\partial}{\partial x_2}[f(x_1, x_2)p(x_1, x_2)] - \frac{g^2 S}{2}\frac{\partial^2 p(x_1, x_2)}{\partial x_2^2} = 0, \tag{15}$$

where $\{x_1, x_2\} \in \Re^2$ is state vector and $p = p(x_1, x_2)$.

For the sliding base-isolation system, the PDF $p(x_1, x_2)$ of the stationary responses must fulfill the following conditions:

$$p(x_1, x_2) \geqslant 0, \quad (x_1, x_2) \in \Re^2,$$

$$\lim_{x_i \to \infty} p(x_1, x_2) = 0, \quad i = 1, 2,$$

$$\int_{-\infty}^{+\infty}\int_{-\infty}^{+\infty} p(x_1, x_2)\,\mathrm{d}x_1\,\mathrm{d}x_2 = 1. \tag{16}$$

If an approximate PDF denoted as $\tilde{p}(\mathbf{x}; \mathbf{a})$ is used, where $\mathbf{a} \in \Re^{N_p}$ and a_i, $(i = 1, 2, \ldots, N_p)$ are parameters to be determined and N_p is the total number of parameters, it is obvious that conditions (16) should also be fulfilled by the approximate PDF.

The approximate PDF of the stationary responses of this system is assumed as an exponential form

$$\tilde{p}(x_1, x_2; \mathbf{a}) = c\exp^{Q_n(x_1, x_2; \mathbf{a})}, \tag{17}$$

where c is a normalization constant and

$$Q_n(x_1, x_2; \mathbf{a}) = \sum_{i=1}^{n}\sum_{j=0}^{i} a_{ij}x_1^{i-j}x_2^j \tag{18}$$

which is an n-degree polynomial in x_1, x_2. In order to fulfill condition (16), it is assumed that

$$\tilde{p}(x_1, x_2; \mathbf{a}) = 0, \quad i = 1, 2, \{x_1, x_2\} \notin \Omega, \tag{19}$$

where $\Omega = [m_1 - c_1\sigma_1, m_1 + d_1\sigma_1] \times [m_2 - c_2\sigma_2, m_2 + d_2\sigma_2] \subset \Re^2$ in which m_i and σ_i denote the mean value and standard deviation of X_i respectively. $c_i > 0$ and $d_i > 0$ are defined such that $m_i - c_i\sigma_i$ and $m_i + d_i\sigma$ are located in the tails of the PDF of X_i, and the derivatives of PDF with respect to x_i equal zero at $m_i - c_i\sigma_i$ and $m_i + d_i\sigma_1$.

Substituting equation (14) into equation (15) leads to

$$x_2\frac{\partial p}{\partial x_1} - 2[\xi\omega + \mu g\delta(x_2)]p - [2\xi\omega x_2 + \mu g\,\mathrm{sign}(x_2) + \omega^2 x_1]\frac{\partial p}{\partial x_2} - \frac{g^2 S}{2}\frac{\partial^2 p}{\partial x_2^2} = 0, \tag{20}$$

where $\delta(\cdot)$ denotes Dirac's delta function.

Equation (20) cannot be satisfied exactly with $\tilde{p}(x_1, x_2; \mathbf{a})$ because $\tilde{p}$ $(\mathrm{x}_1, \mathrm{x}_2; \mathbf{a})$ is only an approximation of $p(x_1, x_2)$. Substituting $\tilde{p}(x_1, x_2; \mathbf{a})$ for $p(x_1, x_2)$ in equation (20) leads to the following residual error:

$$\Delta(x_1, x_2; \mathbf{a}) = x_2\frac{\partial \tilde{p}}{\partial x_1} - 2[\xi\omega + \mu g\delta(x_2)]\tilde{p} - [2\xi\omega x_2 + \mu g\,\mathrm{sign}(x_2) + \omega^2 x_1]\frac{\partial \tilde{p}}{\partial x_2} - \frac{g^2 S}{2}\frac{\partial^2 \tilde{p}}{\partial x_2^2}. \tag{21}$$

Substituting equation (17) into equation (21) yields

$$\Delta(x_1, x_2; \mathbf{a}) = F(x_1, x_2; \mathbf{a})\tilde{p}(x_1, x_2; \mathbf{a}), \tag{22}$$

where

$$F(x_1, x_2; \mathbf{a}) = x_2\frac{\partial Q_n}{\partial x_1} - [2\xi\omega x_2 + \mu g\,\mathrm{sign}(x_2) + \omega^2 x_1]\frac{\partial Q_n}{\partial x_2}$$
$$-\frac{g^2 S}{2}\left[\frac{\partial^2 Q_n}{\partial x_2^2} + \left(\frac{\partial Q_n}{\partial x_2}\right)^2\right] - 2[\xi\omega + \mu g\delta(x_2)]. \tag{23}$$

Because $\tilde{p}(x_1, x_2; \mathbf{a}) \neq 0$, it is required that $F(x_1, x_2; \mathbf{a}) = 0$ if $\tilde{p}(x_1, x_2; \mathbf{a})$ satisfies equation (20). However, usually $F(x_1, x_2; \mathbf{a}) \neq 0$ because $\tilde{p}(x_1, x_2; \mathbf{a})$ is not equal to $p(x_1, x_2)$. In this case, a set of mutually independent functions $H_k(\mathbf{x})$ which span space $\Re^{N_p}$ can be introduced to make the projection of $F(x_1, x_2; \mathbf{a})$ on $\Re^{N_p}$ vanish, i.e.,

$$\int_{-\infty}^{+\infty}\int_{-\infty}^{+\infty} F(x_1, x_2; \mathbf{a})\,H_k(x_1, x_2)\,\mathrm{d}x_1\,\mathrm{d}x_2 = 0, \quad k = 1, 2, \ldots, N_p \tag{24}$$

or

$$\int_{-\infty}^{+\infty}\int_{-\infty}^{+\infty}\left\{x_2\frac{\partial Q_n}{\partial x_1}-[2\xi\omega x_2+\mu g\,\mathrm{sign}(x_2)+\omega^2 x_1]\frac{\partial Q_n}{\partial x_2}-\frac{g^2 S}{2}\left[\frac{\partial^2 Q_n}{\partial x_2^2}+\left(\frac{\partial Q_n}{\partial x_2}\right)^2\right]\right.$$
$$\left.-2[\xi\omega+\mu g\delta(x_2)]\right\}H_k(x_1,x_2)\,\mathrm{d}x_1\,\mathrm{d}x_2=0,\quad k=1,2,\ldots,N_p. \tag{25}$$

Thus, the reduced FPK equation (20) is satisfied with $\tilde{p}(x_1, x_2; \mathbf{a})$ in the weak sense of integration if $F(x_1, x_2; \mathbf{a})\ H_k(x_1, x_2)$ is integrable in $\Re^2$.

By selecting $H_k(x_1, x_2)$ as

$$x_1^{k-l}x_2^l f_1(x_1)f_2(x_2),\quad k=1,2,\ldots,n,\quad l=0,1,2,\ldots,k \tag{26}$$

such that $F(x_1, x_2; \mathbf{a})\ H_k(x_1, x_2)$ is integrable in $\Re^2$, N_p quadratic non-linear algebraic equations in terms of N_p undetermined parameters can be obtained from equation (25) as follows with $f_1(x_1)$ and $f_2(x_2)$ being selected to be Gaussian:

$$\int_{-\infty}^{+\infty}\int_{-\infty}^{+\infty}\sum_{i=1}^{n}\sum_{j=0}^{i}a_{ij}\left\{(i-j)x_1^{i-j-1}x_2^{j+1}-j\left[2\xi\omega x_1^{i-j}x_2^{j}+\mu g x_1^{i-j}x_2^{j-1}\,\mathrm{sign}(x_2)\right.\right.$$
$$\left.+\omega^2 x_1^{i-j+1}x_2^{j-1}-\frac{g^2S}{2}(j-1)x_1^{i-j}x_2^{j-2}\right]$$
$$\left.-\frac{g^2S}{2}\sum_{q=1}^{n}\sum_{r=0}^{q}a_{qr}jr x_1^{i-j+q-r}x_2^{j+r-2}\right\}x_1^{k-l}x_2^l f_1(x_1)f_2(x_2)\,\mathrm{d}x_1\,\mathrm{d}x_2$$
$$-\int_{-\infty}^{+\infty}\int_{-\infty}^{+\infty}2[\xi\omega+\mu g\delta(x_2)]x_1^{k-l}x_2^l f_1(x_1)\,f_2(x_2)\,\mathrm{d}x_1\,\mathrm{d}x_2=0,$$
$$k=1,2,\cdot,n;\ \ l=0,1,2,\cdot,k \tag{27}$$

which results in the following quadratic algebraic equations in terms of unknown parameters a_{ij}, $(i = 1, 2, \ldots, n; j = 0, 1, 2, \ldots, i)$:

$$\sum_{i=1}^{n}\sum_{j=0}^{i}\sum_{q=1}^{n}\sum_{r=0}^{q}\alpha_{ijqr}^{kl}a_{ij}a_{qr}+\sum_{i=1}^{n}\sum_{j=0}^{i}\beta_{ij}^{kl}a_{ij}+\gamma^{kl}=0, \tag{28}$$
$$k=1,2,\cdot,n,\quad l=0,1,2,\cdot,k,$$

where

$$\alpha_{ijqr}^{kl}=-\frac{g^2S}{2}jr I_1^{i+q-j-r+k-l}I_2^{j+r+l-2}, \tag{29}$$

$$\beta_{ij}^{kl}=(i-j)I_1^{i-j+k-l-1}I_1^{j+l+1}-j[I_1^{i-j+k-l}(2\xi\omega I_2^{j+l}+\mu g I_3^{j+l-1})$$
$$+\omega^2 I_1^{i-j+k-l+1}I_2^{j+l-1}-\frac{g^2S}{2}(j-1)I_1^{i-j+k-l}I_2^{j+l-2}], \tag{30}$$

$$\gamma^{kl}=-\,I_1^{k-l}2(\xi\omega I_2^l+\mu g I_4^l) \tag{31}$$

and

$$I_1^m=\int_{-\infty}^{+\infty}x_1^m f_1(x_1)\,\mathrm{d}x_1,\qquad I_2^m=\int_{-\infty}^{+\infty}x_2^m f_2(x_2)\,\mathrm{d}x_2, \tag{32, 33}$$

$$I_3^m = \int_{-\infty}^{+\infty} x_2^m \operatorname{sign}(x_2) f_2(x_2)\, dx_2, \qquad I_4^m = \int_{-\infty}^{+\infty} x_2^m \delta(x_2) f_2(x_2)\, dx_2,$$

$$m = 0, 1, 2, \ldots . \tag{34, 35}$$

The unknown parameters can then be determined by solving equation (28).

The above outlines the procedure for the PDF solution of the system responses with local weighted residual method. It is apparent from the above derivation that the sliding behavior of the structure is not simplified while in the equivalent linearization procedure, the sliding term is incorporated as part of the damping force. Therefore, better results can be expected with local weighted residual method.

5. NUMERICAL ANALYSIS

To assess the effectiveness of the local weighted residual method for a sliding isolation system, the PDF solutions of the system were obtained with the equivalent linearization procedure, the local weighted residual method and Monte Carlo simulation in the present study. A system with $\xi = 0{\cdot}1$, $\omega = 2$ rad/s, $\mu = 0{\cdot}1$ subjected to a weak and a strong excitation is considered respectively. Taking the reference of $S = 0{\cdot}0348\ \mathrm{m^2/s^3}$ ($= 2\pi \times 0{\cdot}005544\ \mathrm{m^2/s^3}$) corresponding to the intensity of the N00W component of El Centro 1940 earthquake as suggested by Bycroft [14], $S = 0{\cdot}01\ \mathrm{m^2/s^3}$ and $S = 0{\cdot}05\ \mathrm{m^2/s^3}$ are chosen for the cases of weak and strong excitations respectively.

5.1. WEAK EXCITATION

For weak excitation with $S = 0{\cdot}01$, the PDFs obtained with the equivalent linearization procedure and the local weighted residual method for $n = 6$ are compared with those obtained with 2×10^7 simulated realizations and shown in Figures 1 and 2. The results

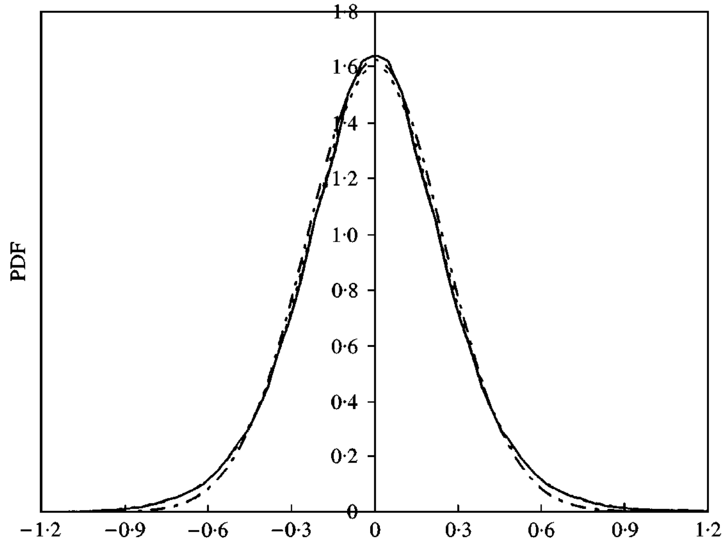

Figure 1. PDFs of the displacement X, weak excitation. —— Simulation; ---- $n = 6$; ——— $n = 2$.

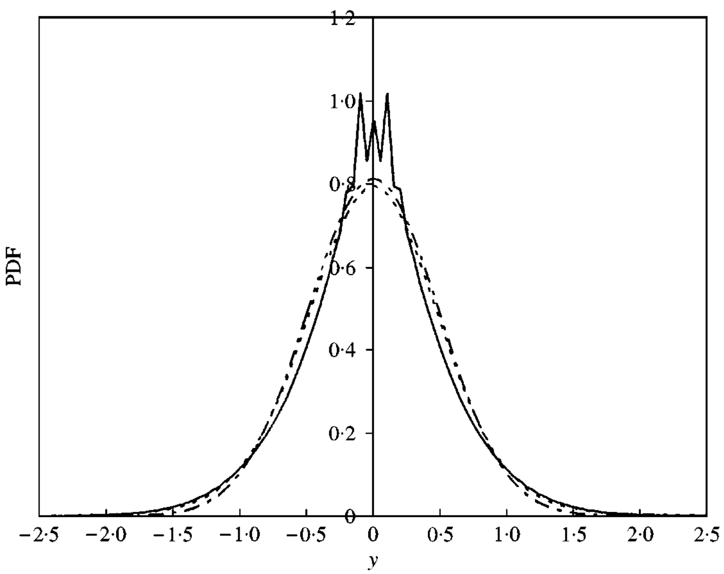

Figure 2. PDFs of the velocity $\dot{X}$, weak ground motion. —— Simulation; ---- $n = 6$; — — — $n = 2$.

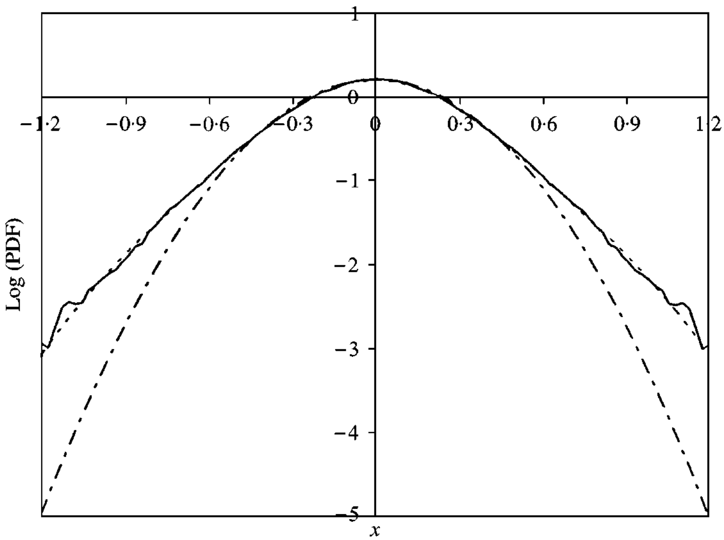

Figure 3. Logarithmic PDFs of the displacement X, weak ground motion. —— Simulation; ---- $n = 6$; — — — $n = 2$.

showed the superiority of the local weighted residual method over the equivalent linearization procedure for the PDFs of both displacement and velocity of the base-isolation system. In Figures 1 and 2, the PDF of displacement is close to Gaussian PDF and the PDF of velocity is also close to Gaussian PDF except in the range around origin. In fact, the PDFs of both displacement and velocity of the base-isolation system are far from being Gaussian, which can be observed from the plots of logarithmic PDFs of responses. The logarithmic PDFs of both displacement and velocity of the base-isolation system are also plotted and compared in Figures 3 and 4 to show the tail behavior of PDFs. It is apparent

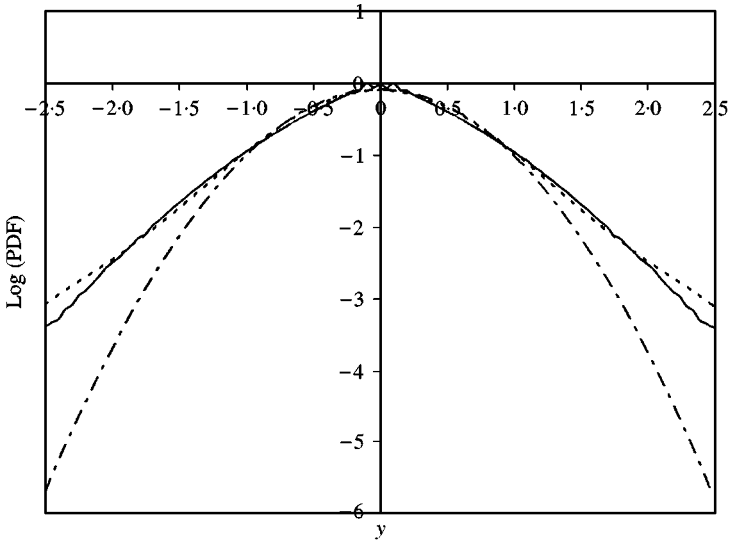

Figure 4. Logarithmic PDFs of the velocity $\dot{X}$, weak ground motion. —— Simulation; ---- $n = 6$; — — — $n = 2$.

that the values in the tails of PDFs obtained with the local weighted residual method agree well with the simulated results, while those from the equivalent linearization procedure deviate from simulated results significantly. Thus, it is concluded that the PDF solutions of both displacement and velocity of the base-isolation system are far from being Gaussian and much more accurate PDF solutions can be obtained with the local weighted residual method.

Moments are also important statistics of system responses; therefore, the moments obtained with different methods are shown and compared in Table 1. It is seen from Table 1 that the moments obtained with the local weighted residual method for $n = 6$ are much improved compared to those obtained with the equivalent linearization procedure which is found to be only suitable for the second moment evaluation if the obtained values of the second moment are acceptable. With the weighted residual method, the higher order moment is more improved than the lower order moment.

5.2. STRONG EXCITATION

Next, we consider a case for strong excitation with $S = 0{\cdot}05\ \mathrm{m}^2/\mathrm{s}^3$ to test the effectiveness of the local weighted residual method for the base isolation system. The PDFs obtained by the local weighted residual method, the equivalent linearization procedure and Monte Carlo simulation of 2×10^7 simulated realizations are shown and compared in Figures 5 and 6. In Figures 5 and 6, the PDFs of both displacement and velocity of the base-isolation system still seem to be of the Gaussian type while the PDFs for $n = 6$ are improved compared to those obtained by the equivalent linearization procedure. In order to compare the tail behavior of PDFs, the logarithmic PDFs are shown and compared in Figures 7 and 8. Similar improved results for $n = 6$ can be observed in the figures. It is also observed that the PDFs in the case of strong excitation are closer to the Gaussian type than the PDFs in the case of weak excitation. In other words, the friction-type base-isolation system can be more linear under the action of stronger excitation.

TABLE 1

Moments for $S = 0{\cdot}01\ \mathrm{m^2/s^3}$

Order	Simulation	Local weighted residual method ($n = 6$)	Linearization
Moments of displacement X			
2	$7{\cdot}107 \times 10^{-2}$	$7{\cdot}162 \times 10^{-2}$	$6{\cdot}024 \times 10^{-2}$
4	$1{\cdot}847 \times 10^{-2}$	$1{\cdot}847 \times 10^{-2}$	$1{\cdot}088 \times 10^{-2}$
6	$9{\cdot}088 \times 10^{-3}$	$8{\cdot}848 \times 10^{-3}$	$3{\cdot}275 \times 10^{-3}$
8	$6{\cdot}363 \times 10^{-3}$	$6{\cdot}065 \times 10^{-3}$	$1{\cdot}377 \times 10^{-3}$
10	$5{\cdot}604 \times 10^{-3}$	$5{\cdot}152 \times 10^{-3}$	$7{\cdot}411 \times 10^{-4}$
12	$5{\cdot}638 \times 10^{-3}$	$5{\cdot}005 \times 10^{-3}$	$4{\cdot}829 \times 10^{-4}$
Moments of velocity $\dot{X}$			
2	$2{\cdot}803 \times 10^{-1}$	$2{\cdot}908 \times 10^{-1}$	$2{\cdot}409 \times 10^{-1}$
4	$3{\cdot}106 \times 10^{-1}$	$3{\cdot}172 \times 10^{-1}$	$1{\cdot}742 \times 10^{-1}$
6	$6{\cdot}307 \times 10^{-1}$	$6{\cdot}892 \times 10^{-1}$	$2{\cdot}097 \times 10^{-1}$
8	1·824	2·234	$3{\cdot}533 \times 10^{-1}$
10	6·585	9·033	$7{\cdot}632 \times 10^{-1}$
12	$2{\cdot}744 \times 10^{1}$	$4{\cdot}138 \times 10^{1}$	2·004

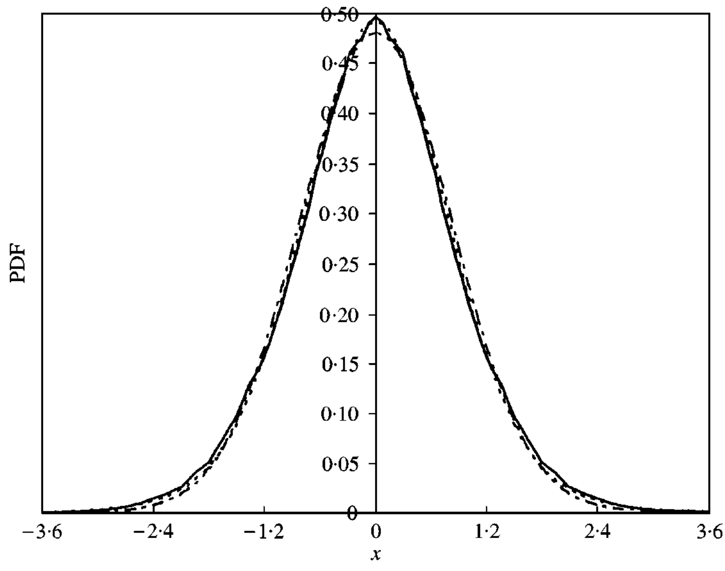

Figure 5. PDFs of the displacement X, strong ground motion. —— Simulation; - - - - $n = 6$; — — — $n = 2$.

In the case of strong excitation, the moments are listed in Table 2. Good improvements are observed for the results obtained by the local weighted residual method compared to those obtained with the equivalent linearization procedure, especially for higher moments. It is also found that the equivalent linearization procedure is only suitable for the evaluation of the second moment even in the case of strong excitation if the obtained values of the second moment are acceptable.

For structural reliability analysis, good prediction of tail behavior of PDFs is very important. From the above numerical analysis, it is observed that the local weighted

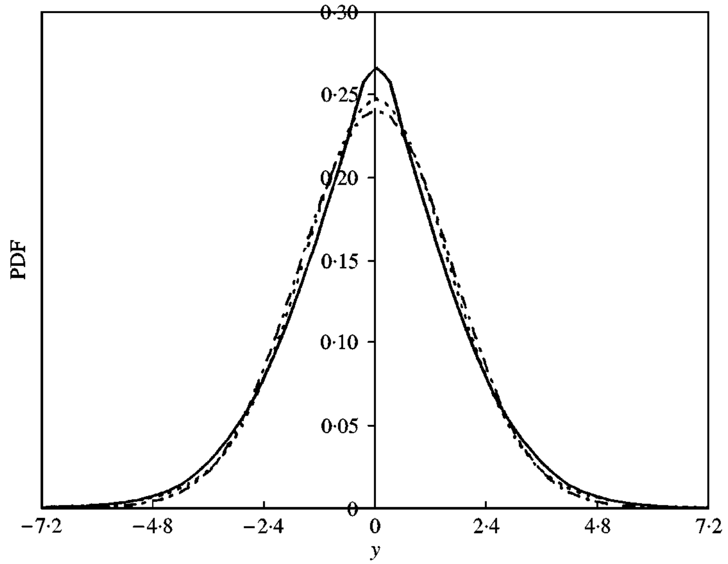

Figure 6. PDFs of the velocity $\dot{X}$, strong ground motion. —— Simulation; ---- $n = 6$; ——— $n = 2$.

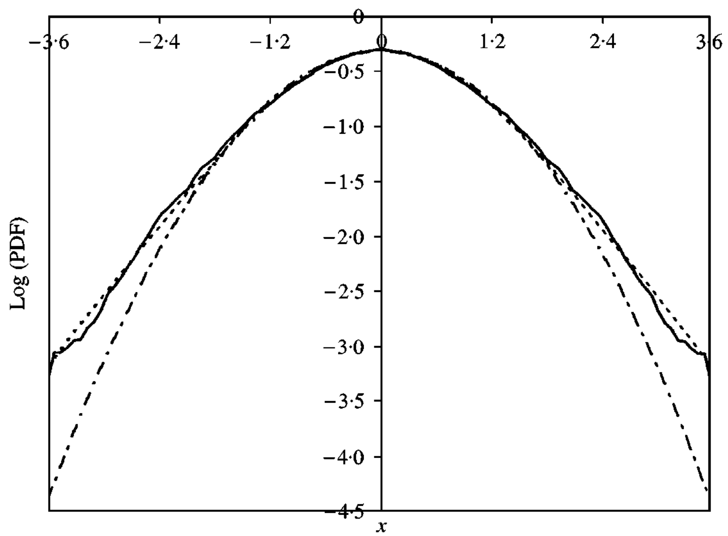

Figure 7. Logarithmic PDFs of the displacement X, strong ground motion. —— Simulation; ---- $n = 6$; ——— $n = 2$.

residual method provides an effective tool for estimating more accurate PDF solutions of the Coulomb friction-type base-isolation system, particularly in the tails of PDFs.

From the figures, it is also observed that the Coulomb friction-type base-isolation system is of "softening" non-linearity (which produces broader tails than the Gaussian PDF) rather than "hardening" non-linearity (which produces narrow tails). Hence, the presented results also validate the applicability of the local weighted residual method for the systems with "softening" non-linearity which poses difficulty for other methods.

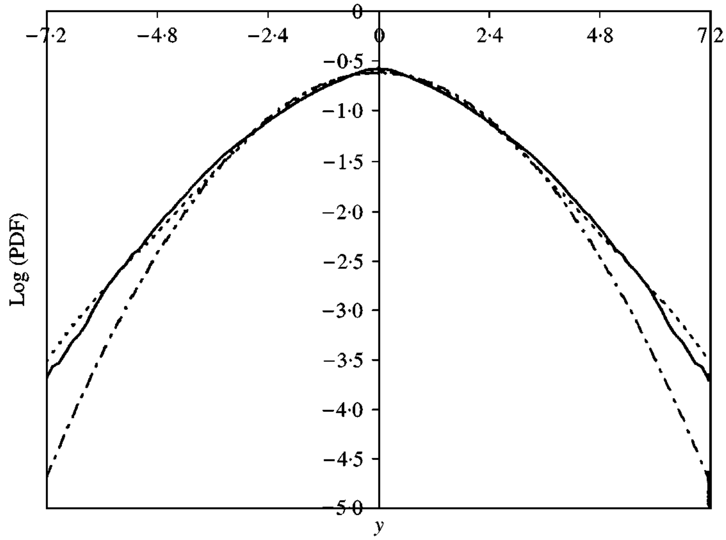

Figure 8. Logarithmic PDFs of the velocity $\dot{X}$, strong ground motion. —— Simulation; - - - - $n = 6$; — — — $n = 2$.

TABLE 2

Moments for $S = 0{\cdot}05\ \mathrm{m^2/s^3}$

Order	Simulation	Local weighted residual method ($n = 6$)	Linearization
Moments of displacement X			
2	$7{\cdot}725 \times 10^{-1}$	$7{\cdot}410 \times 10^{-1}$	$6{\cdot}890 \times 10^{-1}$
4	2·004	1·908	1·422
6	9·019	8·937	4·873
8	$5{\cdot}654 \times 10^{1}$	$5{\cdot}919 \times 10^{1}$	$2{\cdot}313 \times 10^{1}$
10	$4{\cdot}388 \times 10^{2}$	$4{\cdot}810 \times 10^{2}$	$1{\cdot}385 \times 10^{2}$
12	$3{\cdot}916 \times 10^{3}$	$4{\cdot}427 \times 10^{3}$	$9{\cdot}832 \times 10^{2}$
Moments of velocity $\dot{X}$			
2	3·087	2·961	2·756
4	$3{\cdot}264 \times 10^{1}$	$3{\cdot}080 \times 10^{1}$	$2{\cdot}276 \times 10^{1}$
6	$5{\cdot}873 \times 10^{2}$	$5{\cdot}826 \times 10^{2}$	$3{\cdot}119 \times 10^{2}$
8	$1{\cdot}446 \times 10^{4}$	$1{\cdot}549 \times 10^{4}$	$5{\cdot}921 \times 10^{3}$
10	$4{\cdot}350 \times 10^{5}$	$5{\cdot}029 \times 10^{5}$	$1{\cdot}418 \times 10^{5}$
12	$1{\cdot}497 \times 10^{7}$	$1{\cdot}844 \times 10^{7}$	$4{\cdot}027 \times 10^{6}$

6. CONCLUSIONS

Through numerical testing on the local weighted residual method, it is observed that the method is suitable for the probability density analysis of a sliding system with Coulomb friction. For $n = 6$, the obtained PDFs of both displacement and velocity are very close to the results obtained by Monte Carlo simulation. It was also shown that the PDF and the higher (greater than second) order moments obtained with the equivalent linearization procedure are not acceptable for the sliding system, especially in the tails of the PDF which are important for reliability analysis.

The analysis of the PDFs of displacements for different levels of excitation showed that the excitation level is a major factor which influences the PDF types of displacement and velocity of the base-isolation system. It is found that the PDF solutions of both displacement and velocity are closer to the Gaussian type as the power spectral density of excitation increases.

The numerical results show that the base-isolation system with the Coulomb type of friction is of "softening" non-linearity and the local weighted residual method is also effective for such systems with "softening" non-linearity.

Because of the softness of the Coulomb friction-type base-isolation system, the results from the equivalent linearization procedure underestimate in probability the responses of the base-isolation system, which may lead to reliability overestimation. Meanwhile, the local weighted residual method can provide more reliable results.

ACKNOWLEDGMENTS

The results presented in this paper were obtained in the course of research supported by the funding of the Research Committee of the University of Macau, Grant No. 1952/98/UM.

REFERENCES

1. J. M. KELLY 1986 *Soil Dynamics and Earthquake Engineering* **5**, 202–216. Seismic base isolation: review and bibliography.
2. M. C. CONSTANTINOU, J. CACCESE and H. G. HARRIS 1987 *Earthquake Engineering and Structural Dynamics* **15**, 751–759. Frictional characteristics of Teflon–steel interfaces under dynamic conditions.
3. A. MOKHA, M. C. CONSTANTINOU and A. M. REINHORN 1990 *ASCE Journal of Structural Engineerng* **116**, 438–454. Teflon bearings in base isolation. Part 1: testing.
4. M. C. CONSTANTINOU, A. MOKHA and A. M. REINHORN 1990 *ASCE Journal of Structural Engineering* **116**, 455–474. Teflon bearings in base isolation. Part 2: modeling.
5. T. K. CRANDALL, S. S. LEE and J. H. WILLIAMS 1974 *ASME Journal of Applied Mechanics* **41**, 1094–1098. Accumulated slip of a friction-controlled mass excited by earthquake motions.
6. N. MOSTAGHEL and M. KHODAVERDIAN 1987 *Earthquake Engineering and Structural Dynamics* **15**, 379–390. Dynamics of resilient-friction base isolator (R-FBI).
7. L. SU, G. AHMADI and I. G. TADJBAKHSH 1990 *Probabilistic Engineering Mechanics* **5**, 35–46. Responses of basic-isolated shear beam structures to random excitations.
8. M. C. CONSTANTINOU and A. S. PAPAGEORGIOU 1990 *Probabilistic Engineering Mechanics* **5**, 27–33. Stochastic response of practical sliding isolation systems.
9. A. S. PAPAGEORGIOU and M. C. CONSTANTINOU 1990 *Probabilistic Engineering Mechanics* **5**, 19–26. Response of sliding structures with restoring force to stochastic excitation.
10. B. C. LIN, I. G. TADJBAKHSH, A. S. PAPAGEORGIOU and G. AHMADI 1990 *ASCE Journal of Engineering Mechanics* **116**, 446–461. Performance of earthquake isolation systems.
11. G. K. ER 1998 *Proceedings of* 12*th ASCE Engineering Mechanics Specialty Conference*, *San Diego*, *U.S.A.*, 1403–1406. A new nonGaussian closure method for the PDF solution of non-linear random vibrations.
12. G. K. ER 1999 *Journal of Engineering Mechanics* **125**, 443–447. Consistent method for PDF solutions of random oscillators.
13. G. K. ER and V. P. IU 1999 *ASCE Journal of Engineering Mechanics* **125**, 570–574. Probabilistic solutions to nonlinear random ship roll motion.
14. G. N. BYCROFT 1960 *ASCE Journal of Engineering Mechanics* **86**, 1–6. White noise representation of earthquakes.